Figure S1. Related to Figure 1.

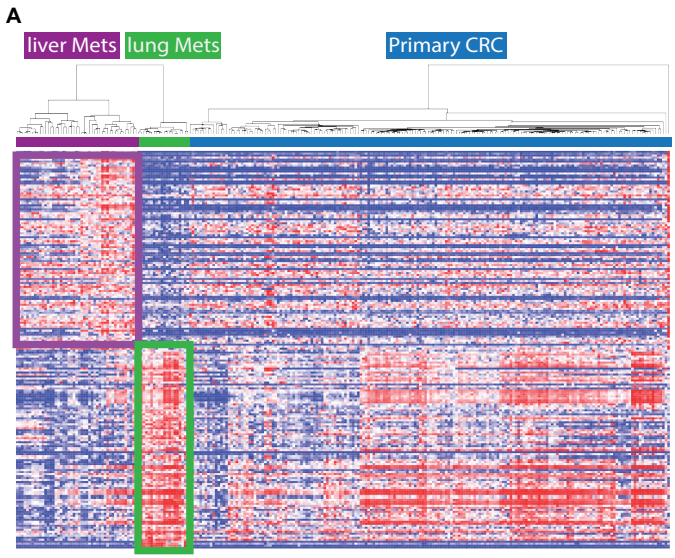

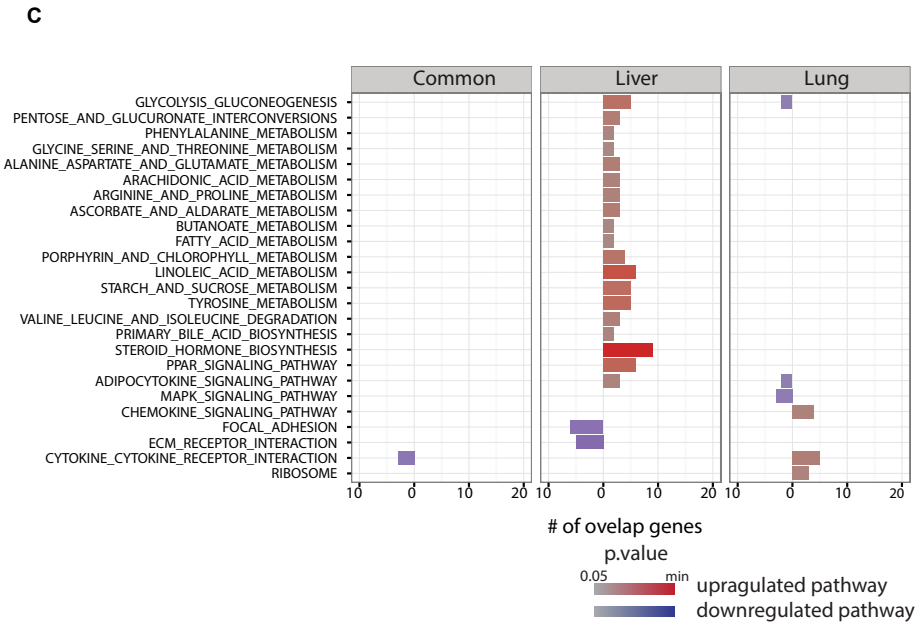

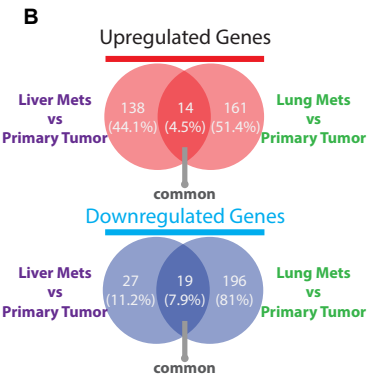

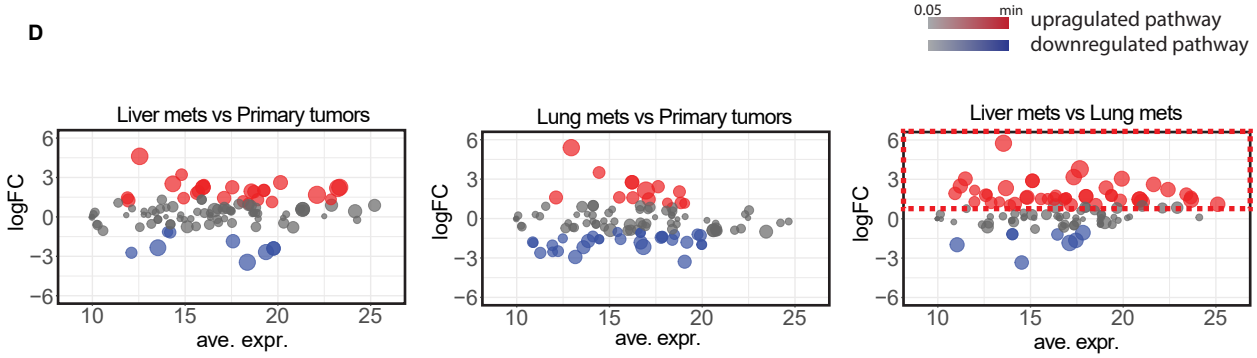

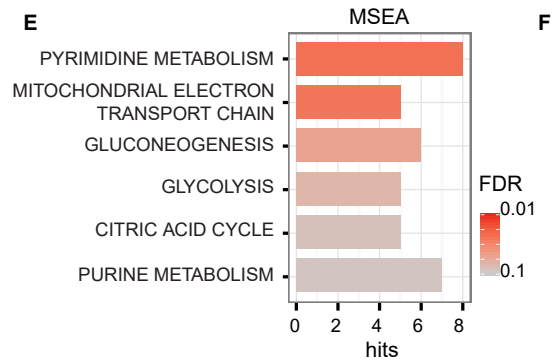

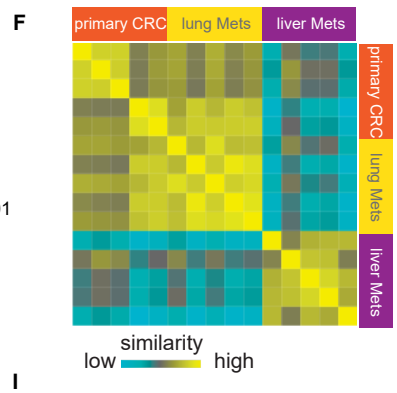

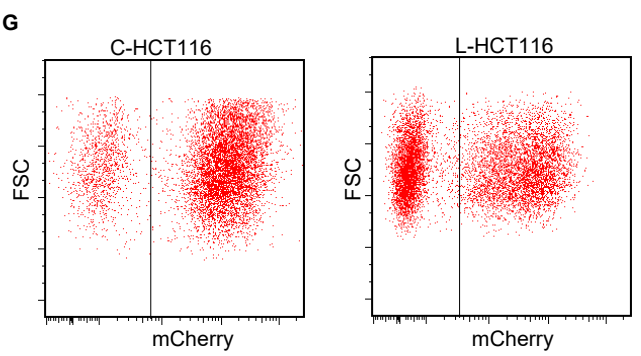

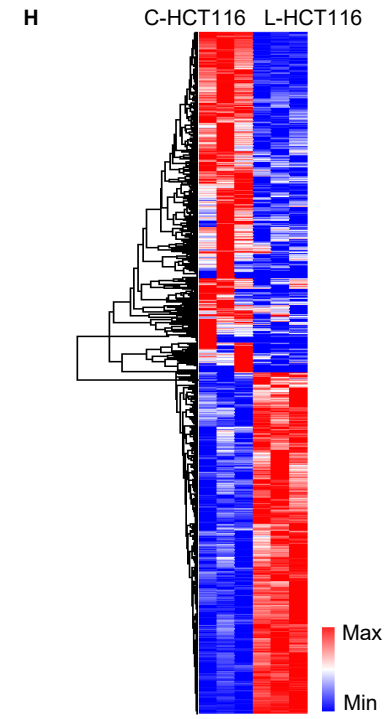

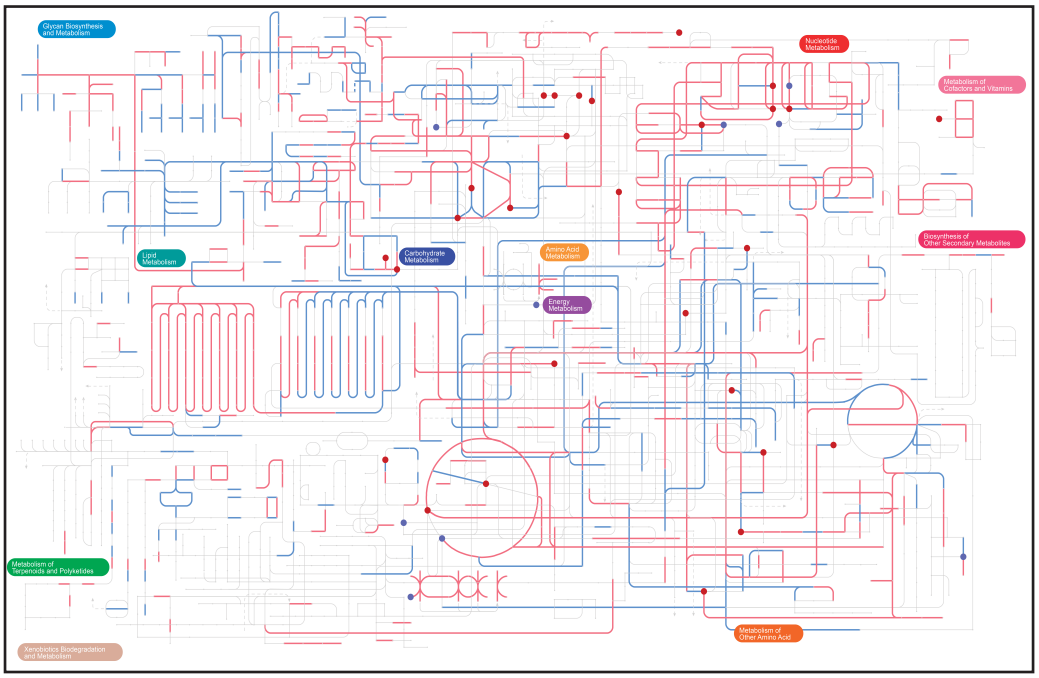

Figure S1. Related to Figure 1.

(**A**) Heatmap of transcriptomic analysis of the GSE41258 dataset including 186 primary tumor samples, 47 liver metastatic samples, and 20 lung metastatic samples from CRC patients. (**B**) Venn Diagram of differential analysis. Top: the significantly upregulated (p value < 0.05, fold change >2) genes in Liver Mets and Lung Mets comparing to primary CRCs. Bottom: the significantly downregulated (p value < 0.05, fold change >2) genes in Liver Mets and Lung Mets comparing to primary CRCs. (**C**) Gene Set Enrichment Analysis. Each panel shows the pathway analysis of the upregulated (red) or downregulated genes (blue) in liver metastases only, lung metastases only, and commonly altered genes respectively. (**D**) MA plots of Liver metastases vs primary tumors (left), lung metastases vs primary tumors (middle), and liver metastases vs lung metastases (right) based on differential analysis. Each dot represents a compound. Colored dots are differentially regulated (p value < 0.05) compounds: Red, upregulation (logFC >1); blue, downregulation (logFC < -1). The radius of the dot is associated with p value—larger dots correspond to smaller p values. (**E**) Metabolite Set Enrichment Analysis (MSEA) comparing liver and lung metastases using MetaboloAnalyst. The metabolites sets shown were filtered based on p value < 0.05 and FDR <0.1. Hits refer to the number of compounds overlapping with the compounds list in the pathways. (**F**) Similarity matrix analysis of metabolite clustering on the metabolomics of primary colon tumors, lung metastases and liver metastases. The similarity matrix is based on Euclidean distance analysis to evaluate the metabolomics difference between samples using Morpheus. (**G**) Representative FACS plots isolating mCherry+ HCT116 cells from primary cecum tumors and liver metastases. (**H**) Heatmap of RNA-seq analysis from isolated cells in (G). (**I**) Comprehensive enrichment metabolic map. The differential (p value < 0.05) genes from RNA-seq and differential metabolites from metabolomics were integrated and shown in the comprehensive metabolic map using iPath2 (Letunic et al., 2008) based on KEGG metabolic map. Dots represent compounds; lines represent the enzymatic genes involved in the metabolic reactions; red represents upregulation; blue represents downregulation.

Figure S2. Related to Figure 2.

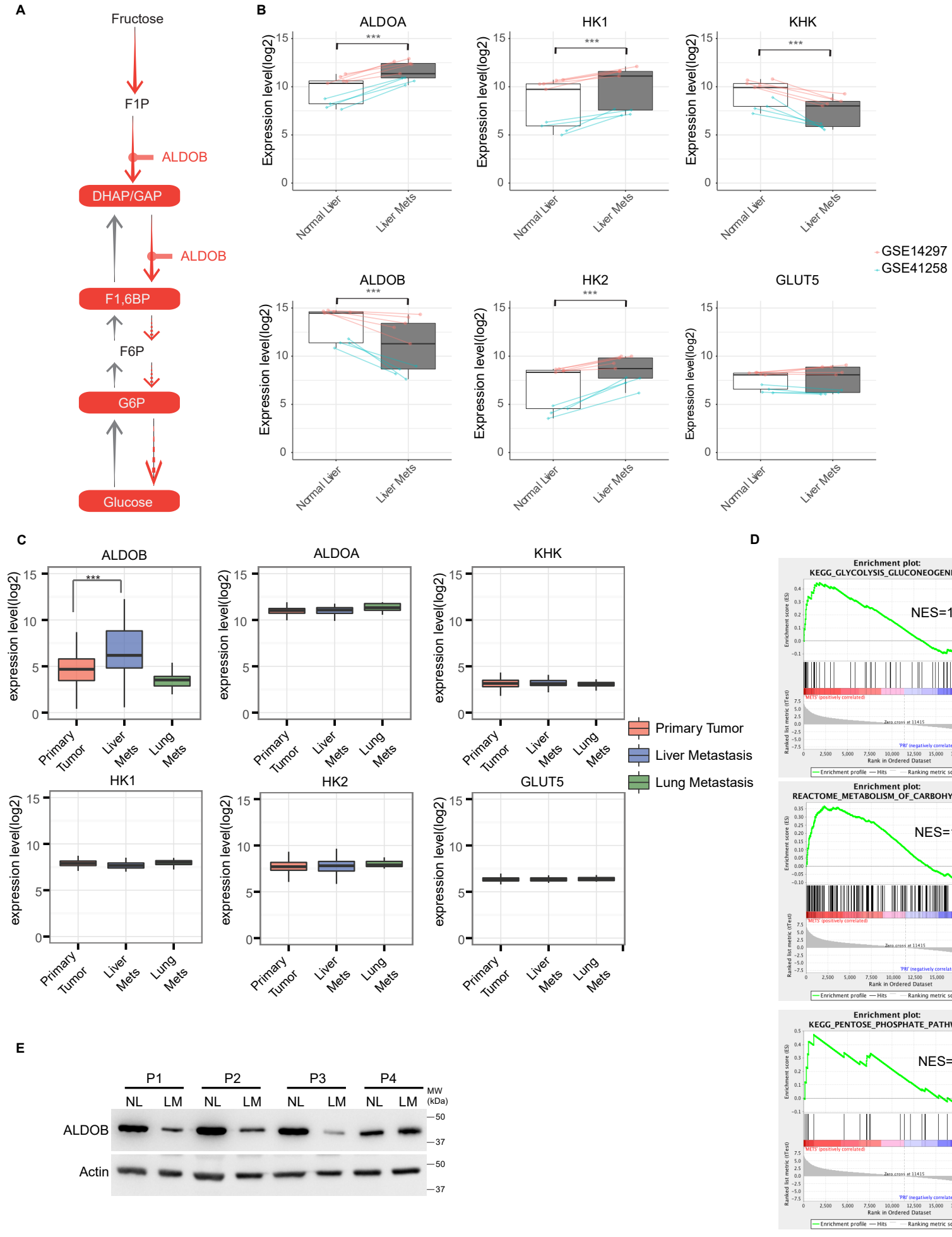

Figure S2. Related to Figure 2.

(**A**) Diagram of ALDOB in fructose metabolism. (**B**) Paired box plots comparing expression levels of ALDOB, ALDOA, KHK, HK1, HK2 and GLUT5 between 9 matched normal liver and liver metastasis tissues in GSE41258 and GSE14297. (**C**) Box plots comparing expression levels of ALDOB, ALDOA, KHK, HK1, HK2 and GLUT5 in the GEO dataset (GSE41258) including 186 primary tumor samples, 47 liver metastatic samples, and 20 lung metastatic samples from colorectal cancer patients. (**D**) GSEA of genes up-regulated in microarray data analysis on 39 primary colon carcinoma and 74 liver metastasis samples from stage IV CRC patients. ***, $p<0.001$. (**E**) Western blots of ALDOB levels in matched normal liver and liver metastasis tissues collected from 4 patients (Table S3B).

Figure S3. Related to Figure 3 and Figure 4.

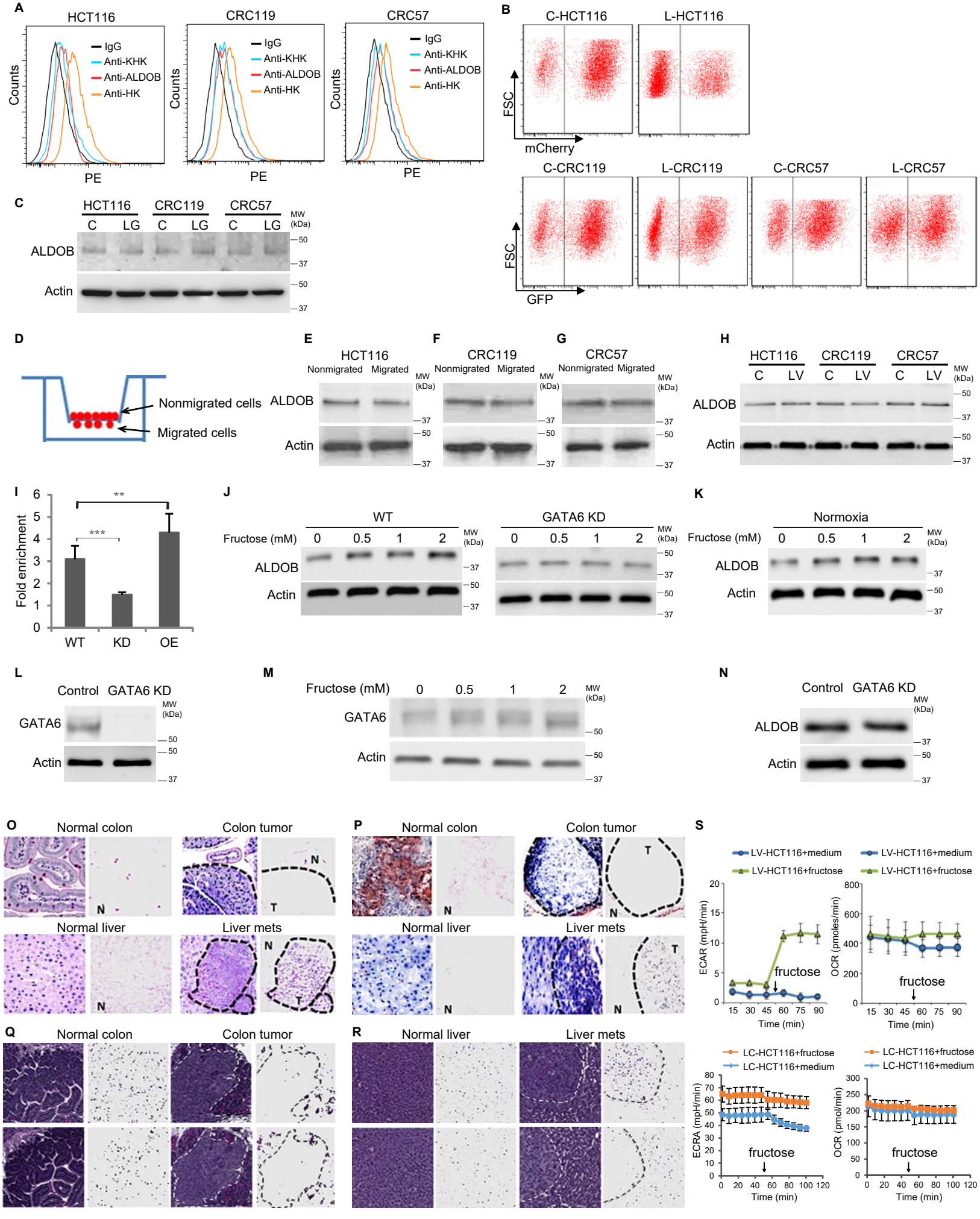

Figure S3. Related to Figure 3 and Figure 4.

(A) FACS plots of ALDOB, KHK, and HK levels in HCT116, CRC119 and CRC57 cells. (**B**) Representative FACS plots of isolating HCT116, CRC119 and CRC57 cells from primary cecum tumor or liver tumors based on fluorescence. (**C**) Western blots of ALDOB levels in CRC cells isolated from primary cecum tumor (C) and lung metastases (LG). (**D**) Schematic of the trans-well migration assay. (**E-G**) Western blot showing ALDOB expression in migrated and non-migrating HCT116 (**E**), CRC119 (**F**) and CRC57 (**G**) CRC cells. (**H**) Western blots of ALDOB levels in CRC cells isolated from primary cecum tumor (C) and liver metastases (LV) after culturing in vitro for 3 days. (**I**) ChIP-qPCR in GATA6 knockdown (KD), ectopic expression (OE) and control (WT) cells showing specificity of GATA6 antibody. Signals were normalized with Actin (input). The fold changes were calculated by normalized with IgG control antibody. Error bars denote s.d. of triplicates. **, $p<0.01$; ***, $p<0.001$. (**J**) Western blot showing upregulation of ALDOB in response to 0-2 mM fructose is dependent on GATA6 in hypoxia. (**K**) Western blot showing ALDOB expression (WT) in 0-2 mM fructose in normoxia. (**L**) Western blot showing GATA6 knockdown efficiency. (**M**) Western blot showing GATA6 expression in response to 0-2 mM of fructose. (**N**) Western blot showing GATA6 did not regulate ALDOB expression in glucose basal medium. (**O**) Periodic Acid Schiff (PAS, magenta color) staining of normal colon, colon tumor, normal liver and liver metastases harvested from HCT116 cells tumor-bearing mice. (**P**) Oil Red O (ORO, red color) staining of normal colon, colon tumor, normal liver and liver metastases harvested from HCT116 cells tumor-bearing mice. (**Q** and **R**) PAS staining coupled with amylase digestion. Hematoxylin and Eosin staining of normal and tumor tissues harvested from tumor-bearing mice. Top: PAS staining; bottom: AS staining coupled with amylase digestion. (**S**) Seahorse assay measuring ECAR and OCR in HCT116 cells derived from liver metastases (LV) or cecum tumors (LC) at baseline and following injection of 11mM Fructose.

Figure S4. Related to Figure 4.

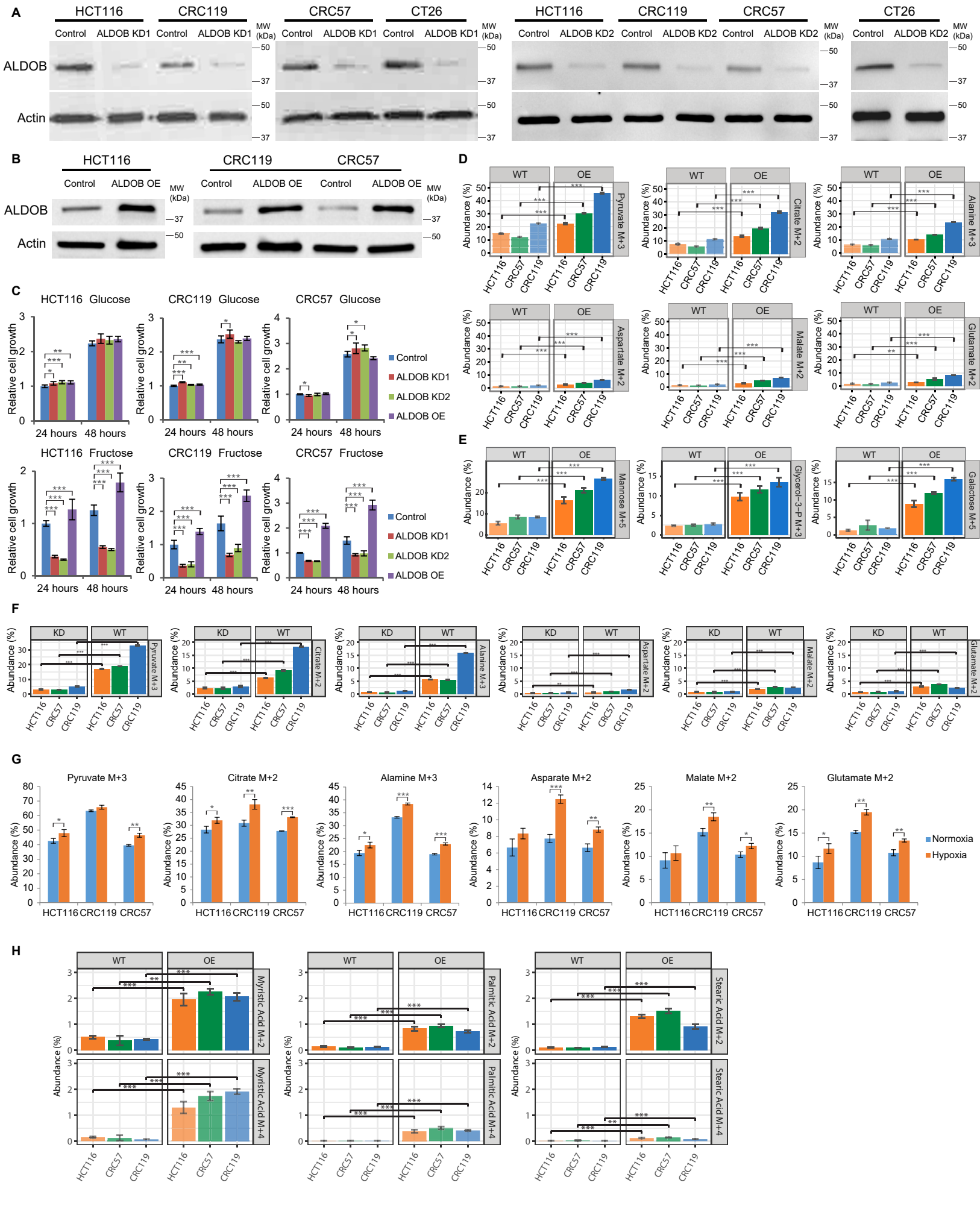

Figure S4. Related to Figure 4

(**A**) Western blot showing ALDOB knockdown efficiency by two shRNAs (ALDOB KD1 and ALDOB KD2) in HCT116, CRC119, CRC57 and CT26 cells. (**B**) Western blot showing ALDOB overexpression efficiency via ectopically expressed ALDOB (ALDOB OE) in HCT116, CRC119 and CRC57 cells. (**C**) WST-1 assay showing the proliferation rates of HCT116, CRC119 and CRC57 cells with control, ALDOB KD, and ALDOB OE. Error bars denote s.d. of triplicates. p-values were calculated based on one-way ANOVA. *, $p<0.05$; **, $p<0.01$; ***, $p<0.001$. (**D**) ^{13}C-labeled carbon was analyzed by GC-MS after cells were incubated in media containing ^{13}C-labeled fructose and dialyzed FBS for 9 hours. WT and OE indicate ALDOB levels in wild type and over expression. (**E**) Labeling of sugar monomers. (**F**) Isotopic tracing analysis with ^{13}C-labeled fructose in ALDOB knockdown cells. ^{13}C-labeled carbon was analyzed by GC-MS with ^{13}C-labeled fructose and dialyzed FBS. (**G**) Isotopic tracing analysis of ^{13}C-labeled fructose in CRC cells in normoxia and hypoxia. (**H**) Tracing analysis of fatty acids in wild-type and ALDOB OE cells cultured in medium containing ^{13}C-labeled fructose. Error bars denote s.d. of triplicates. p-values were calculated based on Student's t-test. *, $p<0.05$; **, $p<0.01$; ***, $p<0.001$.

Figure S5. Related to Figure 5 and Figure 6.

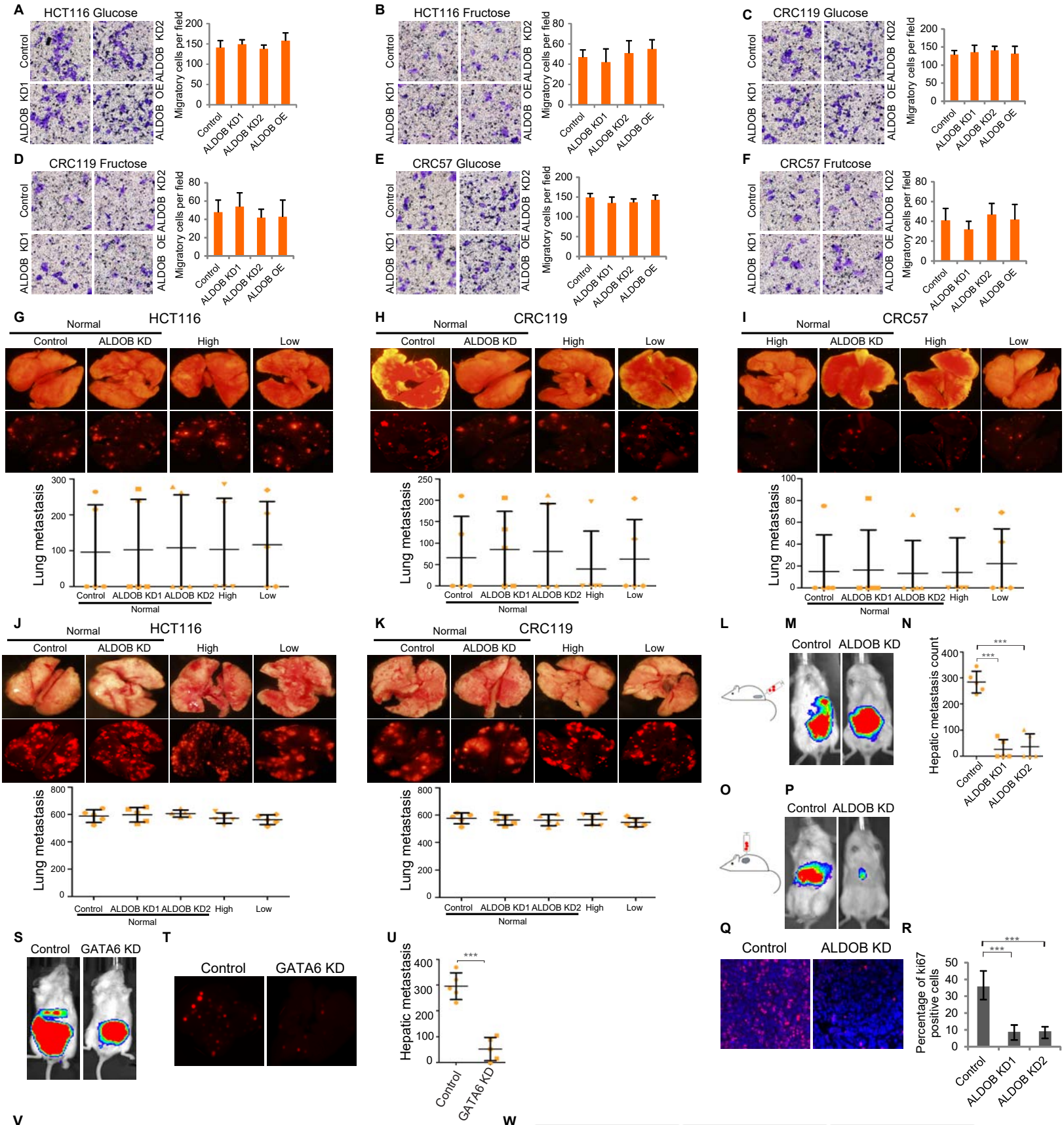

GEO	Gene.symbol	LogFC	p.value	Adj.p.value
GSE14297 GSE35834 GSE41258 GSE49355	GATA6	-0.01	9.29E -01	9.74E -01
GSE41568	GATA6	-0.02	7.90E -01	9.24E -01

Figure S5. Related to Figure 5 and Figure 6.

(**A-F**) Trans-well migration assay showing migration rates of HCT116 (A, B), CRC119 (C, D) and CRC57 (E, F) cells with control, ALDOB KD, and ALDOB OE in glucose- or fructose-containing medium. Error bars denote s.d. of triplicates. p-values were calculated based on one-way ANOVA. *, $p<0.05$; **, $p<0.01$; ***, $p<0.001$. (**G-I**) Analysis of CRC lung metastasis with cecum injection of HCT116 cells (G), CRC119 cells (H) and CRC57 cells (I), with ALDOB knockdown (ALDOB KD1 and ALDOB KD2), or fructose-high (High) or fructose-restricted-diet (Low). (**J** and **K**) Analysis of CRC lung metastasis with tail vein injection of HCT116 cells (J), CRC119 cells (K), with ALDOB knockdown (ALDOB KD1 and ALDOB KD2), or fructose-high (High) or fructose-restricted diet (Low). Error bars denote s.d. of 5 mice per group. (**L**) Schematic of cecum injection. (**M** and **N**) Analysis of CRC liver metastasis in BALB/c mice with cecum injection of CT26 cells. Knockdown of ALDOB suppressed liver metastasis in immunocompetent BALB/c mice. (**O**) Schematic of intrahepatic injection. (**P**) Representative IVS images showing knockdown of ALDOB suppressed CT26 cell growth in the liver. (**Q** and **R**) Ki-67 staining showing knockdown of ALDOB suppressed CT26 cell proliferation in the liver. (**S-U**) Representative IVIS luciferase *in vivo* images (S), fluorescent images of livers (T), and quantification of liver metastasis (U) showing GATA6 knockdown suppressed liver metastasis in cecum-injection mouse model. Error bars denote s.d. of 5 mice per group. ***, $p<0.001$. (**V**) GATA6 expression between primary CRC and liver metastases in GSE14297, GSE35834, GSE41258, and GSE49355 (matched tissues) and GSE41568 (unmatched tissues). (**W**) Correlation analysis between ALDOB and GATA6 in the GEO datasets.

Figue S6. Related to Figure 5, Figure 6 and Discussion.

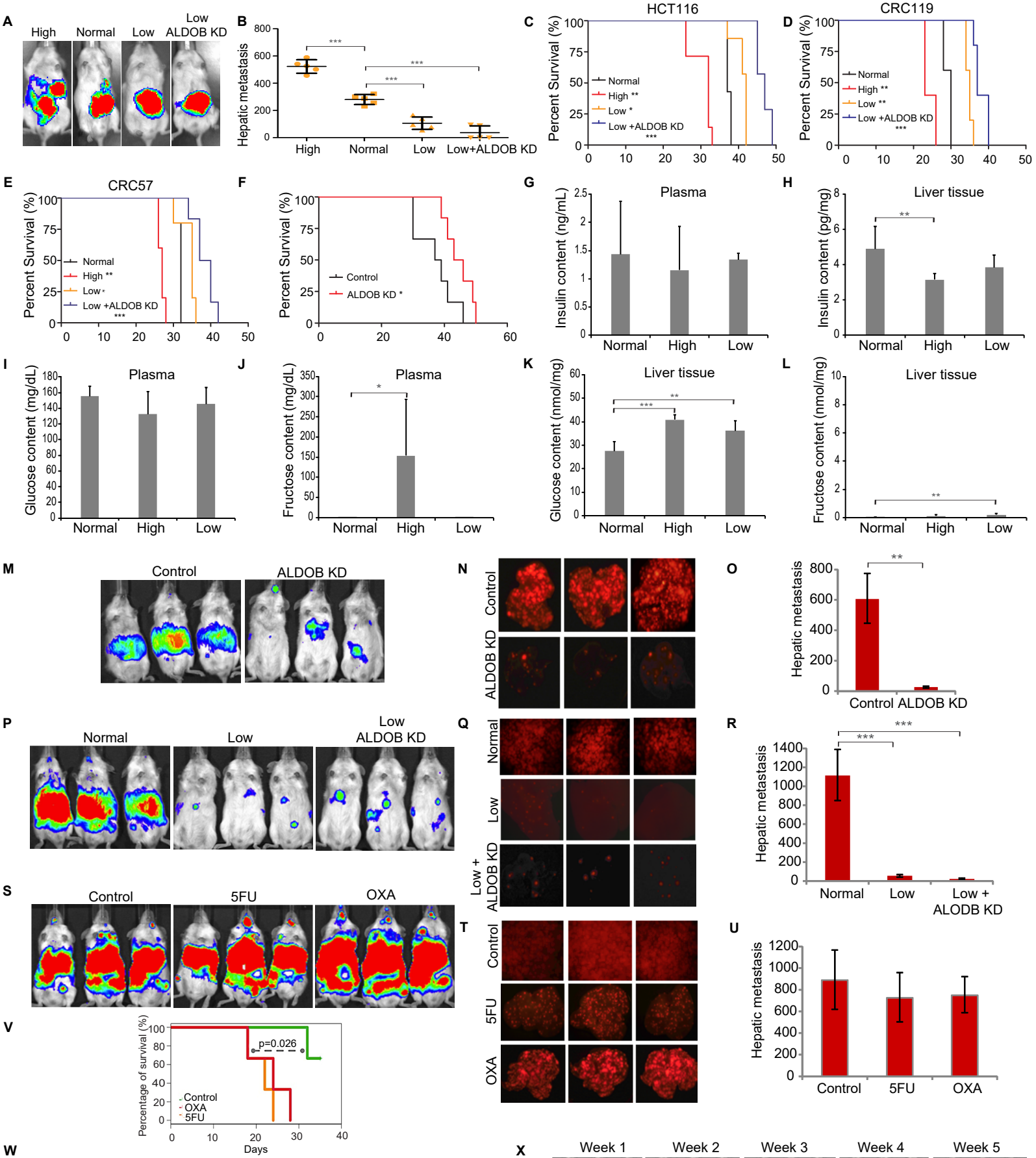

W

GEO ID	Primary tumor site	Metastatic site	Gene	LogFC	P.Value	# of primary tumor	# of metastatic tumor
GSE46141	Breast Cancer	liver	ALDOB	5.49	2.82E-09	11	16
GSE56493	Breast Cancer	liver	ALDOB	4.70	3.27E-09	27	19
GSE2741	Breast Cancer	liver	ALDOB	1.87	1.18E-08	46	3
GSE71729	Pancreatic ductal adenocarcinoma	liver	ALDOB	3.85	1.72E-15	145	25
GSE42952	Pancreatic ductal adenocarcinoma	liver	ALDOB	1.08	3.91E-04	12	7

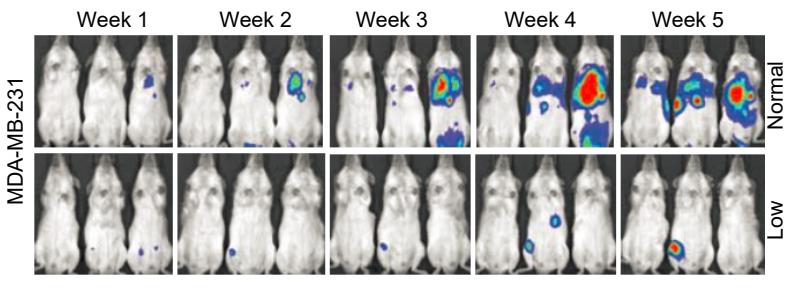

Figure S6. Related to Figure 5, Figure 6 and Discussion.

(**A-B**) Impact of fructose restriction in an immunocompetent model. Cecum injection of CT26 cells showing fructose-high diet (High) promoted liver metastasis, while fructose-restricted diet with ALDOB knockdown (Low+ALDOB KD) suppressed liver metastasis in immunocompetent BALB/c mice. Error bars denote s.d. of 5 mice per group. p-values were calculated based on one-way ANOVA. **, $p<0.01$; ***, $p<0.001$. (**C-E**) Survival curves of mice with cecum injection fed with a regular diet (Normal), a fructose-high diet (High), a fructose-restricted diet (Low), or a fructose-restricted diet+ALDOB knockdown (Low+ALDOB KD). (**F**) Survival curves of mice with intrahepatic injection of control or ALDOB knockdown HCT116 cells fed with a regular diet. p value was calculated in comparison with normal diet group on the base of log-rank test. *, $p<0.05$, **, $p<0.01$; ***, $p<0.001$. (**G** and **H)** Insulin content in plasma (G) and liver tissue (H) of mice fed with a regular diet (Normal), a fructose-high diet (High), a fructose-restricted diet (Low). **(I-L**) Glucose (I) and fructose (J) content in plasma as well as glucose (K) and fructose (L) content in liver tissue of mice fed with a regular diet (Normal), a fructose-high diet (High), a fructose-restricted diet (Low). Error bars denote s.d. of 5 mice samples per group. p-values were calculated based on one-way ANOVA. *, $p<0.05$; **, $p<0.01$; ***, $p<0.001$. (**M-O**) Analysis of mice with intravenous injection of liver-derived HCT116 cells with or without ALDOB knockdown. Representative IVIS luciferase *in vivo* images (M), fluorescent (mCherry) images of livers (N) and quantification of liver metastasis (O) show knockdown of ALDOB suppressed CRC liver lesions. (**P-R**) Analysis of mice with intravenous injection of liver-derived HCT116 with fructose diet. Representative IVIS luciferase *in vivo* images (P), fluorescent (mCherry) images of livers (Q) and quantification of liver metastasis (R) show mice fed with fructose-restricted diet (Low) suppressed liver lesions. (**S**) Representative images of mice injected with liver metastasis derived mCherry labeled HCT116 and treated with normal saline (Control), 5-Fluorouracil (5FU, 100mg/kg), or Oxaliplatin (OXA, 6mg/kg). (**T**) Fluorescent imaging of liver tissue from mice in (S). (**U**) quantification of liver lesions. (**V**) Survival curve analysis of treated and untreated tumor-bearing mice from (S). Error bars denote s.d. of 3 mice per group. **, $p<0.01$; ***, $p<0.001$. p-value was calculated based on one-way ANOVA. (**W**) ALDOB expression between primary breast cancer and liver metastases as well as primary pancreatic cancer and liver metastases in available GEO datasets. (**X**) Intravenous injection mouse models showing MDA-MB-231 breast cancer cell liver metastasis in mice fed with a regular diet (Normal) or a fructose-restricted diet (Low).

Table S1. Related to Figure 1 and Figure 2.

S1A. Information of NCBI:GEO databases used in this study.

Title	Platform	GEO ID	Normal colon	Primary CRC	Liver mets
Expression Profile of Primary Colorectal Cancers and associated Liver Metastases	Illumina human-6 v2.0 expression beadchip	GSE14297	7 (7)	18 (7)	18 (7)
Impact of miRNAs modulation on regulatory networks and pathways involved in colon cancer and metastasis development	[HuEx-1_0-st] Affymetrix Human Exon 1.0 ST Array	GSE35834	23 (9)	30 (9)	27 (9)
Expression data from colorectal cancer patients	[HG-U133A] Affymetrix Human Genome U133A Array	GSE41258	54 (4)	186 (4)	47 (4)
Specific extracellular matrix remodeling signature of colon hepatic metastases	[HG-U133A] Affymetrix Human Genome U133A Array	GSE49355	18 (10)	20 (10)	19 (10)

( ): number of matched samples

S1B. Integrated analysis of primary colon tumor and liver metastases

Pathways	Metabolites	Genes
Fructose/mannose metabolism	Glycerone phosphate; Lactate; beta-D-Fructose 1,6-bisphosphate	GMPPB; HK1; HK2; MPI; PFKFB2; PFKFB3; PFKFB4; PFKL; PFKM; PFKP; PMM2; ENOSF1; TIGAR; SORD; TPI1; TSTA3; FBP1; ALDOB; ALDOC; HK3; KHK
Pentose Phosphate Pathway	Glucose; Glucono-1,5-lactone; Gluconic acid; 6-Phospho-D-gluconate; beta-D-Fructose 1,6-bisphosphate; Sedoheptulose 7-phosphate	GLYCTK; RPIA; PGLS; GPI; DERA; PFKL; PFKM; PFKP; PGD; PGM2; PRPS1; PRPS2; TALDO1; FBP1; ALDOB; ALDOC
Glycolysis/Gluconeogenesis	Glucose; Glycerone phosphate; Lactate; beta-D-Fructose 1,6-	DLAT; ENO1; ENO2; ALDH1B1; GPI; HK1; HK2; LDHA; LDHB; PDHA1; PFKL; PFKM; PFKP; PGAM1; PGK1; PGM2; TPI1; ADPGK;

	bisphosphate	LDHAL6B; G6PC3; FBP1; ALDOB; ALDOC; HK3; ADH1A; ADH1B; G6PC; PCK1; ENO3	
Cysteine and methionine metabolism	S-Adenosyl-L-homocysteine; Glutathione; 2-Oxobutanoate; 4-Methylthio-2-oxobutanoic acid	DNMT1; DNMT3A; GOT2; LDHA; LDHB; MDH1; MTAP; MTR; ADI1; ENOPH1; SMS; SRM; MRI1; LDHAL6B; TAT; SDS; BHMT; CDO1; MAT1A	
Valine, leucine and isoleucine degradation	2-Oxobutanoate	ECHS1; ACSF3; ALDH1B1; ACADM; IVD; ACAT2; OXCT1; PCCB; OXCT2; ACADS; ACAA2; ABAT; HMGCS2; ALDH6A1	
Arginine and proline metabolism	Glyoxylate	CKB; ALDH1B1; GAMT; GOT2; PYCR2; MAOB; NOS3; ODC1; LAP3; ALDH18A1; PYCR3; SMS; SRM; GATM; CPS1; GLUL; ALDH4A1; ARG1; P4HA1	
Fatty acid metabolism		CPT1A; ECHS1; HACD2; FASN; MCAT; ACACA; ACADM; ACAT2; FADS1; HACD3; ADH1A; ADH1B; ACADS; ACAA2; ACADVL	
Tryptophan metabolism		ECHS1; ALDH1B1; GCDH; ACAT2; MAOB; OGDH; AADAT; OGDHL; HAAO; TDO2; KMO; KYNU	
Alanine, aspartate and glutamate metabolism	Fumarate; Carbamoyl phosphate	ADSL; ADSS; GLS2; GLS; GLUD1; GOT2; RIMKLA; NAT8L; ASL; PPAT; NIT2; CAD; CPS1; GLUL; ALDH4A1; ABAT	
Glycine, serine and threonine metabolism	Glyoxylate; 2-Oxobutanoate	GLYCTK; GCAT; GAMT; GCSH; MAOB; PGAM1; CHDH; SRR; SHMT2; GATM; SDS; BHMT; GLDC	GLYCTK; GCAT; GAMT; GCSH; MAOB; PGAM1; CHDH; SRR; SHMT2; GATM; SDS; BHMT; GLDC

S1C. Top metabolic genes upregulated in liver mets vs. primary CRCs

Gene.symbol	logFC	P.Value	adj.P.Val
G6PC	2.13	1.26E-04	6.17E-03
ALDOB	2.08	2.70E-05	1.85E-03
ADH1B	2.03	3.11E-06	3.07E-04
HPD	1.88	4.08E-06	3.85E-04
GATM	1.82	8.97E-09	2.65E-06
AOX1	1.80	3.11E-08	7.12E-06

Table S2. Related to Figure 2. Information of CRC patients included in the microarray.

Patient ID	Primary Site	Metastatic Site	Gender	Stage
MET_CRC002D	Colon	Liver	Female	IV
MET_CRC007A	Colon	Liver	Male	IV
MET_CRC011	Colon	Liver	Male	IV
MET_CRC015	Colon	Liver	Female	IV
MET_CRC019	Colon	Liver	Male	IV
MET_CRC021B	Colon	Liver	Male	IV
MET_CRC022	Colon	Liver	Male	IV
MET_CRC024A	Colon	Liver	Female	IV
MET_CRC028A	Colon	Liver	Female	IV
MET_CRC033	Colon	Liver	Male	IV
MET_CRC037A	Colon	Liver	Male	IV
MET_CRC039A	Colon	Liver	Male	IV
MET_CRC040	Colon	Liver	Female	IV
MET_CRC041	Colon	Liver	Male	IV
MET_CRC044	Colon	Liver	Female	IV
MET_CRC045	Colon	Liver	Male	IV
MET_CRC047	Colon	Liver	Male	IV
MET_CRC049	Colon	Liver	Male	IV
MET_CRC050	Colon	Liver	Male	IV
MET_CRC051	Colon	Liver	Male	IV
MET_CRC056	Colon	Liver	Male	IV
MET_CRC057A	Colon	Liver	Male	IV
MET_CRC058	Colon	Liver	Male	IV
MET_CRC060	Colon	Liver	Female	IV
MET_CRC061	Colon	Liver	Female	IV
MET_CRC062	Colon	Liver	Male	IV
MET_CRC063	Colon	Liver	Male	IV

MET_CRC066A	Colon	Liver	Female	IV
MET_CRC002D	Colon	Liver	Female	IV
MET_CRC067A	Colon	Liver	Female	IV
MET_CRC075A	Colon	Liver	Male	IV
MET_CRC077A	Colon	Liver	Male	IV
MET_CRC078A	Colon	Liver	Male	IV
MET_CRC087A	Colon	Liver	Male	IV
MET_CRC089A	Colon	Liver	Male	IV
MET_CRC092	Colon	Liver	Female	IV
MET_CRC094	Colon	Liver	Female	IV
MET_CRC094B	Colon	Liver	-	IV
MET_CRC096	Colon	Liver	Male	IV
MET_CRC097	Colon	Liver	Male	IV
MET_CRC098D	Colon	Liver	Female	IV
MET_CRC102A	Colon	Liver	Female	IV
MET_CRC103	Colon	Liver	Female	IV
MET_CRC103C	Colon	Liver	-	IV
MET_CRC105B	Colon	Liver	Male	IV
MET_CRC107A	Colon	Liver	Male	IV
MET_CRC108	Colon	Liver	Male	IV
MET_CRC109A	Colon	Liver	Female	IV
MET_CRC112	Colon	Liver	Male	IV
MET_CRC118A	Colon	Liver	Female	IV
MET_CRC119A	Colon	Liver	Female	IV
MET_CRC125A	Colon	Liver	Male	IV
MET_CRC128A	Colon	Liver	Male	IV
MET_CRC133A	Colon	Liver	Male	IV
MET_CRC134A	Colon	Liver	Male	IV
MET_CRC145A	Colon	Liver	Male	IV

MET_CRC147A	Colon	Liver	Male	IV
MET_CRC148A	Colon	Liver	Female	IV
MET_CRC149A	Colon	Liver	Male	IV
MET_CRC151A	Colon	Liver	Female	IV
MET_CRC159	Colon	Liver	Male	IV
MET_CRC160A	Colon	Liver	Male	IV
MET_CRC162A	Colon	Liver	Female	IV
MET_CRC165A	Colon	Liver	Female	IV
MET_CRC172A	Colon	Liver	Male	IV
MET_CRC174B	Colon	Liver	Female	IV
MET_CRC221A	Colon	Liver	Male	IV
MET_CRC230A	Colon	Liver	Male	IV
MET_CRC236A	Colon	Liver	Male	IV
MET_CRC241A	Colon	Liver	Female	IV
MET_CRC249A	Colon	Liver	Male	IV
MET_CRC253A	Colon	Liver	Male	IV
MET_CRC261A	Colon	Liver	Male	IV
MET_CRC074A	Rectal	Liver	Female	IV
MET_CRC167	Rectal	Liver	Female	IV

Table S3. Related to Figure 2.
S3A. Differential expression of ALDOB in liver vs primary CRC analyzed on the base of five databases.

Title	GEO ID	# of Liver mets	# of Primary CRC	logFC	p.Value
A Molecular Profile of Colorectal Cancer to Guide Therapy	GSE41568	74	39	3.75	$5.03x10^{-8}$
Expression data from colorectal cancer patients	GSE41258	47	186	2.75	$4.66x10^{-14}$
Expression Profile of Primary Colorectal Cancers and associated Liver Metastases	GSE14297	18	18	1.89	$1.53x10^{-3}$
Impact of miRNAs modulation on regulatory networks and pathways involved in colon cancer and metastasis development	GSE35834	27	30	1.48	$3.22x10^{-4}$
Specific extracellular matrix remodeling signature of colon hepatic metastases	GSE49355	19	20	2.85	$1.56x10^{-4}$

S3B. Information of CRC patients from whom normal liver and liver metastasis tissues were acquired.

Patient ID	Gender	Primary site	Metastatic site	Differentiation	Stage
P1	F	colon	liver	Moderately differentiated	IV
P2	F	colon	liver	Poorly differentiated	IV
P3	F	rectal	liver	Well differentiated	IV
P4	M	colon	liver	Well differentiated	IV

Table S4. Related to Figure 3, 4, 5, 6.
Information of patients who CRC119 and CRC57 cell lines were derived from.

Cell line	Gender	Primary site	Metastatic site	Differentiation	Stage
CRC119	F	colon	liver	moderate	IV
CRC57	M	colon	liver	moderate	IV

Table S5 Related to Figure 6.
Ingredient of fructose-high, fructose-restricted and regular diet.

Ingredient	Diet		
	Fructose-high diet	Fructose-restrict diet	Regular chow diet
kcal/gm	3.8	3.8	3.1
Protein	19%	19%	25%
Carbohydrate	69%	69%	58%
Fat	3%	3%	17%
Casein	200 g	200g	
L-Cystine	3g	3g	
Corn Starch	0	1590g	
Maltodextrin	0	528g	
Sucrose	0	0	
Fructose	720g	0	
Cellulose, BW	50g	50g	
Soybean Oil	30g	30g	
t-Butylhydroquinone	0.014g	0.014g	
Mineral Mix S10022G	35g	35g	
Vitamin Mix V10037	10g	10g	
Choline Bitartrate	2.5g	2.5g	